Chapter 3

The Basic Structure of the Human Liver from the Viewpoint of Vascular Architecture

Let me begin analysis of organ structure with introducing some thoughts about the liver and its microvasculature (Takahashi, 1970; Takahashi and Chiba, 1990; Takahashi *et al.*, 1992). The liver is a voluminous organ comparable in size to the lung, with a microstructure appearing not only quite simple but randomized in terms of orientation with which the blood vessels are arranged. This makes us expect that we would be able to rely on stereological method in various facets of study. However, taking a step into asking what fundamental principle dominates this organ in its structure-function correlation, one may realize the study cannot be that easy. The following is an example showing how much had to be consumed to understand what the "organ structure" implies even in this simple organ.

a) The unitary structure—different concepts

The swine liver: 2-D and 3-D appearance of hepatic lobules (Figs. 3-1, 3-2)

Shown in Fig. 3-1 is a microscopic picture of the liver, not of human but of swine. It seems to be an assembly of well demarcated chambers, each comprising parenchymal tissue. These chambers have been called the hepatic lobules. In the swine, the lobules are separated from the neighboring ones, though not always perfectly, with thin membranes made of connective tissue. At the places where three membranes meet, one can find a mass of collagen which contains a duct space and is usually called a portal tract because it conducts a triad of peripheral portal vein, hepatic artery and bile duct. Though various, the average shape of lobules on a 2-D section is said to be hexagonal, and one can find a portal tract at each of the vertices. Blood flows into the lobule from both the portal vein and hepatic artery, the former bearing more than 90% of the total blood flow. After irrigating the intralobular capillary network, the blood is drained by a small vein, which is found at the center of the lobule and therefore is called the central vein, a headspring of the hepatic vein.

As in the figure, the lobules appear in a 2-D microscopic section as polygons of various shape. This means that 3-dimensionally, lobules are polyhedra packed in the space. Figure 3-2 is a part of swine liver reconstructed with the aid of a computer system. Only an early stage of reconstruction is shown in the figure where a small thickness was reproduced, because with the advancement of reconstruction, the pic-

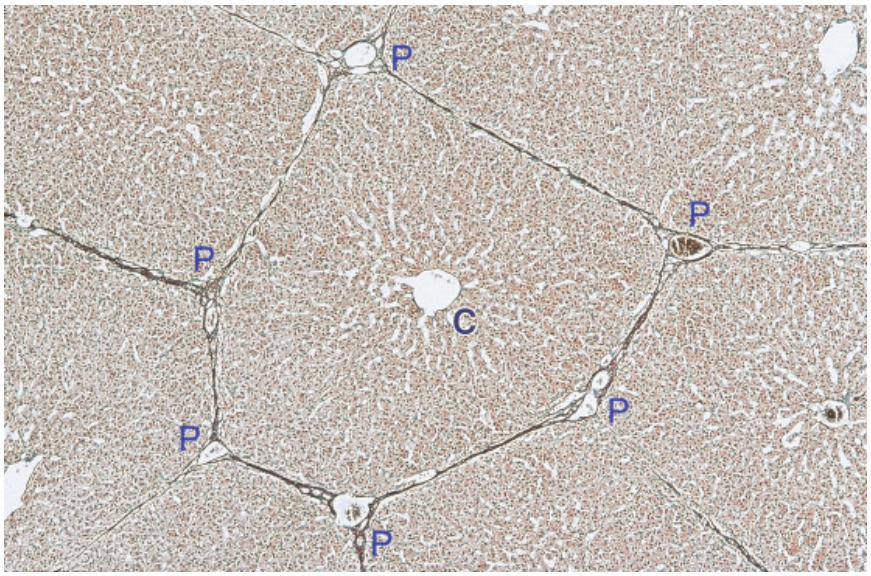

Fig. 3-1. Microscopic appearance of the liver of swine. Clearly, the parenchyma is divided with thin connective tissue septa into polygonal areas which are called the hepatic lobules. Terminal portal veins run through the portal tracts (P). At the center of each lobule, a central vein (C), the terminal segment of hepatic vein, originates and drains blood from the lobule. Gomori's silver stain.

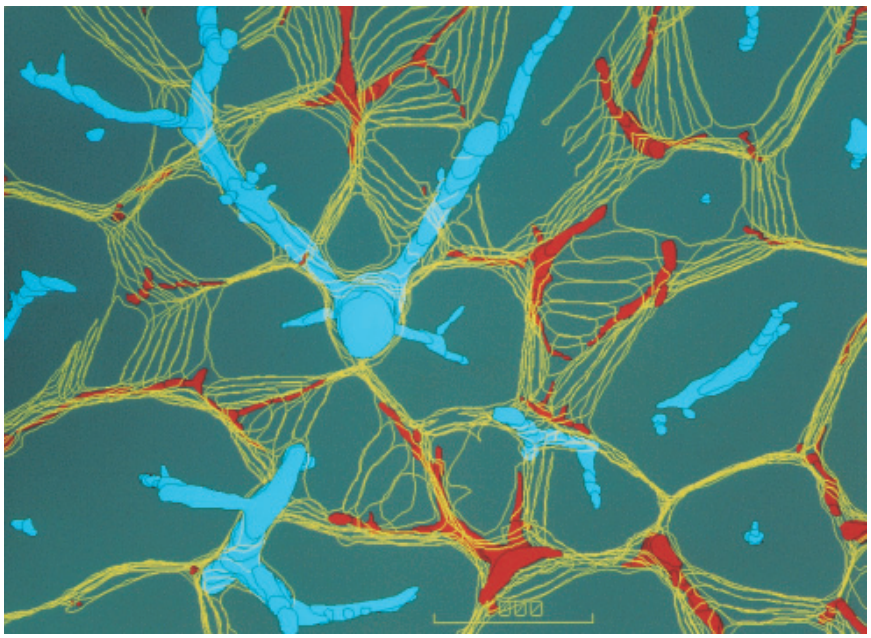

Fig. 3-2. Computer-assisted 3-D reconstruction of swine liver. The yellow wireframes are the interlobular septa, the vessels painted red are portal veins, and those painted blue are hepatic veins. Even in this early stage of reconstruction one can see that the parenchyma consists of polyhedral lobules.

ture becomes growingly complicated, making it hard to keep a clear perspective of the basic structural framework. Still, even at this stage of reconstruction where serial sectional pictures have just started to stack, it may be understood that the space is packed with polyhedral lobules with portal veins (red) running along the interlobular membranes and hepatic veins (blue) penerating the lobules.

Characterization of polyhedral lobules (Figs. 3-3, 3-4)

The geometry of lobular polyhedra was analyzed upon serial sections of swine liver. After the contours of lobules were checked in each of the serial sections as in Fig. 3-3, the sectional pictures were stacked and scanned through over a thickness of 1cm to define the shape of individual lobules. As the result, a total of 56 lobules were confirmed retaining integrity, without being truncated at the margin of the tissue block. Figure 3-4 is a histogram exhibiting the number of faces for the 56 lobular polyhedra. The polyhedra were shown to have varying number of faces, ranging from 8 to 22, but the mean was calculated at 13.7. This is a value close to fourteen, and reminds us that a face number of 14 was given for the average polyhedra, to which animal cells were assimilated (Lewis, 1923, 1933). Suwa (1981) also gave a mean number of 14 for the polyhedra produced by random packing of spheres. Discussing that this corresponds to the space division where the total surface area of polyhedra attains the minimum, he designated this as the equilibrium space division. Although we are far from understanding the physical significance of the lobular geometry, it seems to the author that mainly, the function of the connective tissue septa of the swine liver is a mechanical one. The septa are likely to be holding the lobules as they are, resisting excessive

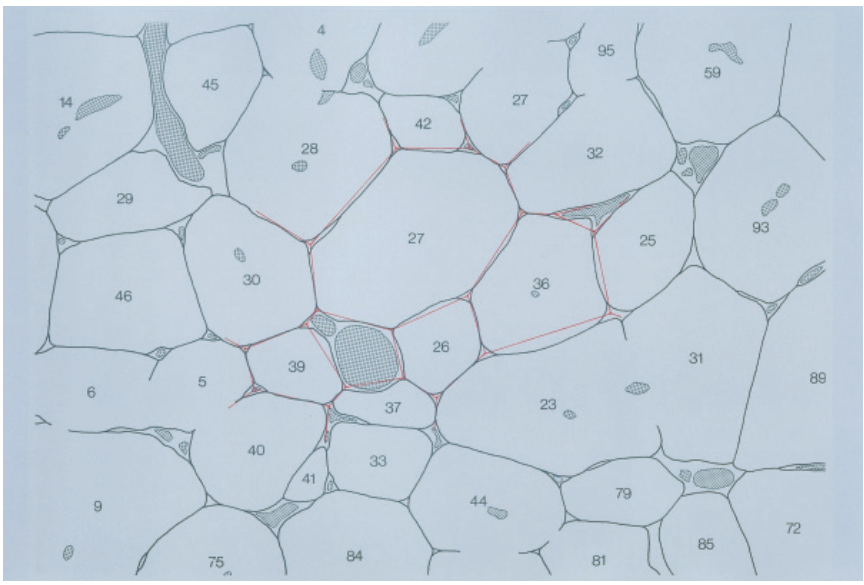

Fig. 3-3. In one of serial sections, the contours of lobules are picked up by tracing, a procedure necessary for the reconstruction of Fig. 3-2. Lobular contours are defined so as to construct a packing of polygons as partially shown by red lines.

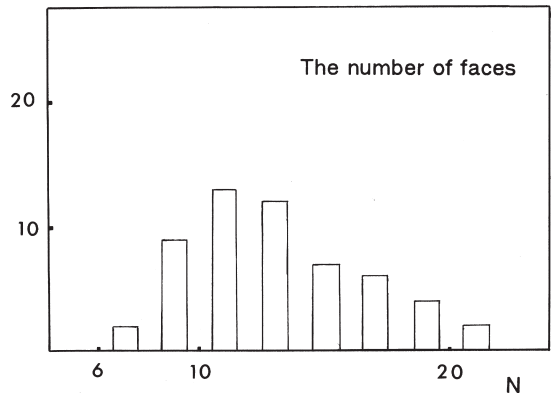

Fig. 3-4. The number of faces N counted for each of the 56 lobules reconstructed from serial sections of swine liver. A mean face number of 13.7 was obtained.

mechanical force exerted upon the liver which is a soft and voluminous organ, susceptible to rupture when too much deformed. From a microcirculation point of view, all the blood that has irrigated a lobule is drained by its central vein. Therefore one can say that functionally, the lobules may also be definable as a unit of venous drainage.

Normal human liver: microphotograph of lobule (Fig. 3-5)

Figure 3-5 is a microscopic picture of normal liver of human. Here one can no longer find such connective tissue septa that in the swine were enveloping the lobules.

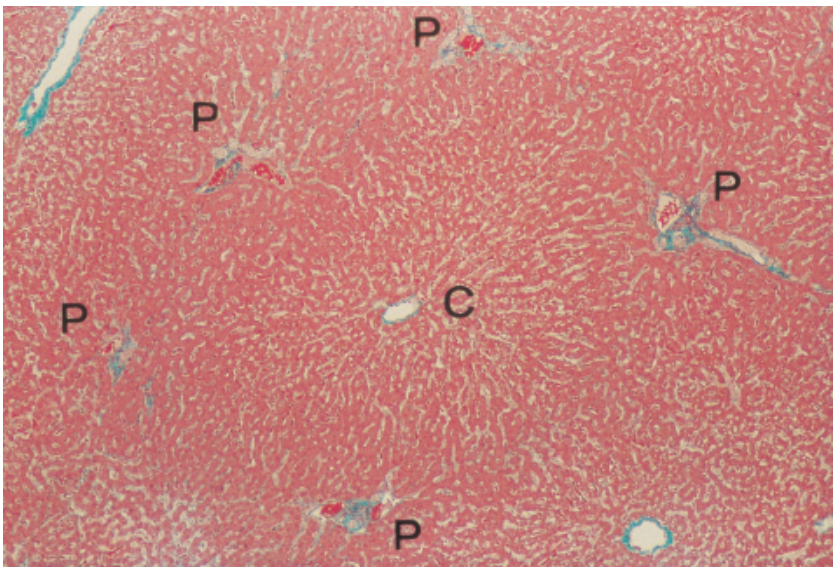

Fig. 3-5. The microscopic appearance of normal human liver. P: the portal tract. C: the central vein. Despite the lack of interlobular septa, arrangement of these vessels exactly reproduces that of the swine liver. Elastica-Goldner stain.

However, there is unmistakably a parenchymal area that may be definable with the portal veins (P) surrounding the area, and with a central vein (C) penetrating the area at the center. The area seems likely to be corresponding to the lobule of the swine liver from which only the septa were taken away, leaving the portal tracts and central veins at the places where they were. Also in the arrangement of lobules in the human liver shown in Fig. 2-36, little difference seems to exist compared with the swine.

The acinar model (Fig. 3-6)

It would have been a matter of course that the lobular concept, as shown above, was widely accepted on account of its easy recognizability. In the early 1950s, however, Rappaport (1954) proposed another unit of the liver based on different concept. Displaying the schema of Fig. 3-6, he maintained that in the human as well as in the other mammals, the fundamental unit of the liver should be defined in the form of what he called an acinus. His unit was schematized as a small parenchymal clump having a terminal portal venule at the center and flanked by terminal hepatic venules, the latter corresponding to the draining vessels which were called the central veins in Figs. 3-1 and 3-5. According to Rappaport (1963), one of the reasons why he prefers this concept to the classic lobule is that in any organ, it should be the afferent vessel that determines the basic framework of the unitary structure. Moreover, he contends, the liver is a glandular organ that secretes bile, where the basic design of gland should be determined by the arrangement of secreting ducts. In fact, the intrahepatic bile ducts run and divide in parallel with the portal veins, and he concludes that in this respect too, the portal tracts have a much greater functional significance than do the hepatic veins.

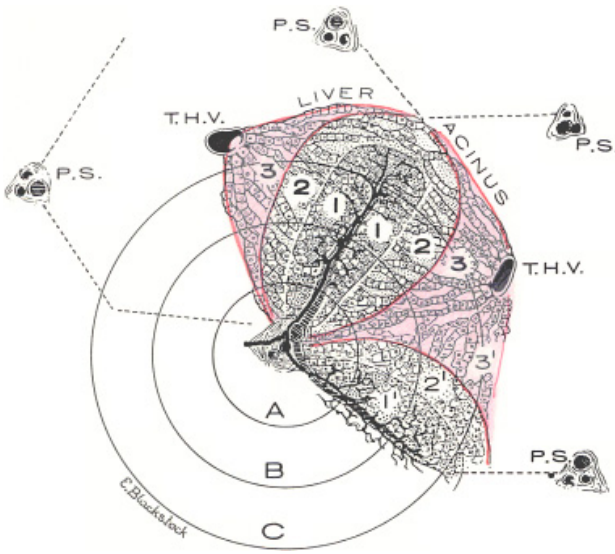

Fig. 3-6. The acinar model. With this schema, Rappaport maintains that the basic structural unit of the liver should be defined as an ellipsoidal mass having a terminal portal venule at the center, which he called the acinus. An acinus is said to comprise three zones, 1, 2 and 3, in which order, blood was assumed to irrigate through an acinus. Reproduced from Rappaport *et al*. (1954): Anat Rec 119, pp. 11.

However, the matter is not that simple. In the first place, one can hardly talk about something like the superiority of the afferent vessel over the efferent one, since microcirculation of an organ may not be sustainable under a malfunctioning efferent vessel, and in this respect the outlets of blood have to be considered equally indispensable with the inlets. In the second place, the liver is indeed an excretory gland producing bile. But structurally, the liver is classified into the type of netlike gland, quite a unique one. Here, bile is secreted into the bile canaliculi which form a vast network continuing over the whole organ, as shown later (Figs. 3-26 and 3-27). At many places, the network is tapped with a terminal bile ductule (the canal of Hering) which leads to an interlobular duct, the peripheral branch of biliary tree. Therefore, even if several terminal ductules came to be obstructed, bile can be drained through any of the other exits. In these circumstances, it may be clear that in the liver where bile can be secreted via any route of the biliary system, one cannot define a glandular lobule in such a way as in ordinary exocrine glands like the pancreas or salivary glands.

In the third place, if the acinar concept were tenable as a functionally significant circulatory unit of the liver, it must be able to explain the morphogenesis of various liver changes developing under impaired circulation, because it has been defined as a unit of tissue blood flow. In the practice of diagnostic pathology, hepatocellular necrosis due to ischemia or intoxication is often experienced. But in reality, the pattern of liver lesions actually found in such patients is far from what one might expect by assuming the acinar concept. This issue will be revisited in Chapter 7.

b) The microvasculature of human liver and its functional significance

Three-D vascular architecture of human liver (Fig. 3-7)

Let us consider the problem, watching the actual 3-D microvasculature of the normal liver. Figure 3-7 is the result of computer-assisted reconstruction of a human liver, and presents the architecture of small blood vessels, with the portal veins painted in pink and the hepatic veins in light blue. The terminal branches of the hepatic vein correspond to the central veins of lobules. One may find small areas surrounded by dots at two places. One of them, Area 1, has a hepatic venule (a central vein) at the center and is circumscribed by several terminal branches of portal vein. Apparently, this represents a single, swine-type lobule. With this in mind, let us trace the portal venules, and we can see that the whole space is separable into similar lobules. On the other hand, an acinus of Rappaport, though hardly recognizable from the arrangement of small vessels in the space, may correspond to something like Area 2, the other small space. Thus, from a microanatomical point of view, the classical lobules are far more clearly definable than Rappaport's acini.

However, let us re-examine the matter from another viewpoint, keeping ourselves from being too much absorbed in the issue of unitary structures. Now, pay attention to the spatial relation between the hepatic (central) venules and the portal venules surrounding them. Then one may see that over the whole area reconstructed, both of the vessels are positioned in the space so as to embrace between them a distance which is kept uniform to a certain degree. However, between a pair of neighboring portal and hepatic venules, any relationship can exist in terms of their mutual angle. Therefore

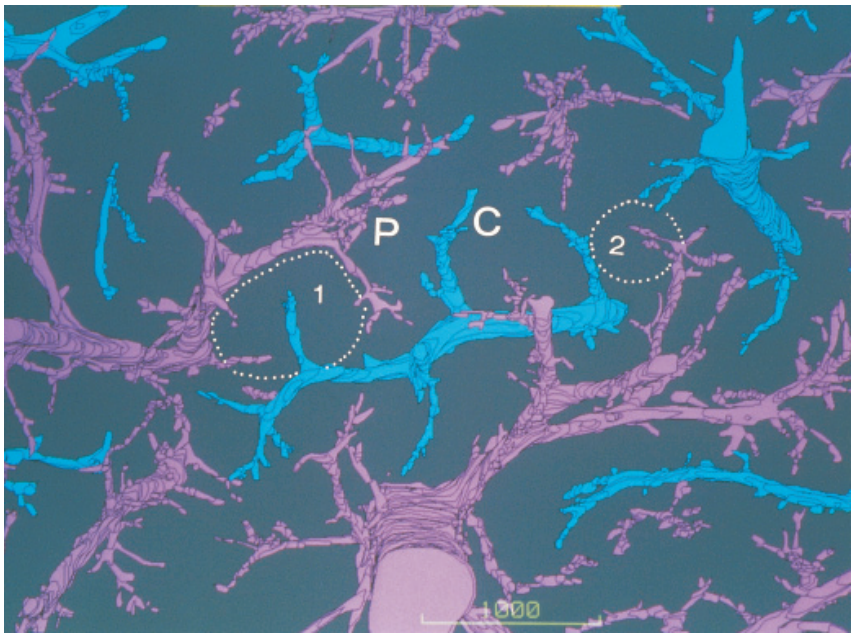

Fig. 3-7. Computer-assisted 3-D reconstruction of the hepatic microvasculature in a normal human liver. Portal veins (P) are painted in pink, and the hepatic veins (C: central vein) in light blue. Note that the terminal portal and hepatic venules are arranged in the space in an isodistant fasion, i.e., so as to embrace a similar distance between them. Two areas are encircled by dots: while Area 1, corresponding to a lobule, is well definable with the surrounding portal venules, an acinus (Area 2) is barely visible from the way the vessels are deployed in the space. Reproduced from Takahashi *et al*. (1990): Science on Form II, pp. 19.

the portal-central-venous distance has to be defined in clearer geometric terms. The definition will be introduced afterwards, and here let us only have an overview by comparing the picture with another organ where the isodistant relationship of vasculature seems to be retained much less than in the liver.

The vasculature of cerebral cortex: difference from the liver (Fig. 3-8)

Shown in Fig. 3-8 for comparison is the microvasculature of human cerebral cortex. This is a reconstruction of small arteries and veins manually performed at a time when computer assist was not available. At a glance, the arrangement of small arteries (non-shaded) and veins (shaded) appears so much complicated and irregular as to suggest that in this organ, the afferent-efferent vascular distance may be less uniform than we saw in the liver.

The interdigitating relationship (Fig. 3-9)

In the hepatic vasculature, the afferent portal and the efferent hepatic venules are arranged alternately in the space as schematized in Fig. 3-9. In anatomy, this relation is expressed as "interdigitation," with which to compare to the fingers of both hands locked together. Also in the cerebral cortex shown in the foregoing figure, one can

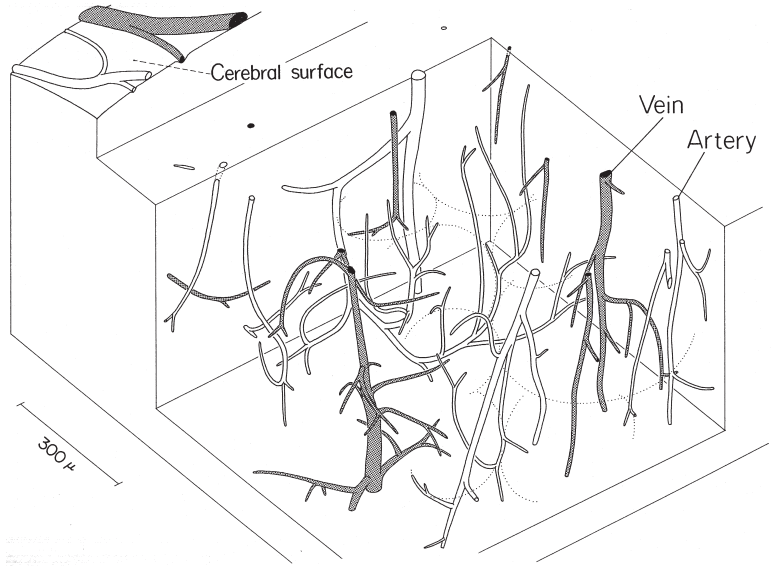

Fig. 3-8. Manually performed 3-D reconstruction of the microvasculature of cerebral cortex. Note the relation of small arteries (white) and veins (shaded). While an "interdigitating" relationship is retained, the pattern is more complicated and irregular than in the liver, with the arterio-venous isodistance not so clearly visible. Reproduced from Takahashi (1970): Tohoku J exp Med 101, pp. 123.

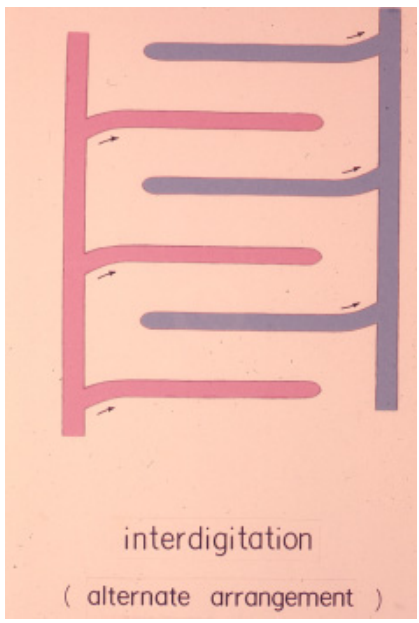

Fig. 3-9. A schema illustrating the "interdigitating" relation of afferent and efferent vessels. In other words, an alternating relation.

find, by closely watching, the interdigitating relation retained in the whole region, allowing to define circulatory "units" around small veins as roughly depicted with dotted circles along their putative borders. Thus, the difference between the liver and the cerebral cortex is that in the former, there exists quite an ***isodistant*** interdigitating vasculature, while in the latter the afferent-efferent vascular distance is much less uniform. As will be shown, the liver has a vasculature that retains the highest isodistance among the organs. If so, what significance does the isodistant vasculature of the liver have in the organ function? Because morphologically, it is the microvasculature that makes the liver a unique organ, it may be reasonable to assume that there may be some uniqueness in the hepatic circulation.

The portal vein: its uniqueness (Figs. 3-10, 3-11)

With respect to circulation, the uniqueness of the liver lies, of course, in that it has the portal vein as its functional afferent vessel. The portal vein is a low pressure vessel, with the blood pressure at the trunk being as low as 8 mmHg, whereas the quantity of blood that flows through this vessel amounts to 1.5 L/min, or 25 to 30% of the cardiac output. This implies that the intrahepatic portal venous tree has to convey and distribute such an amount of blood to the periphery at such a low blood pressure. Figure 3-10 presents the fall of blood pressure theoretically estimated for the portal

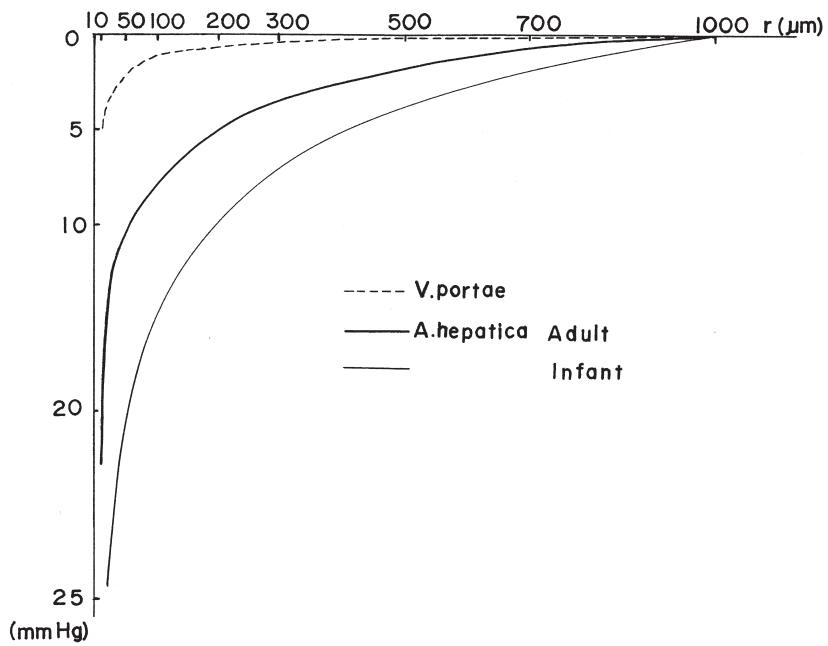

Fig. 3-10. The blood pressure drop is estimated for the intrahepatic portal vein and hepatic artery by measuring the length and radius of segments on a vascular cast and according to the model of Suwa *et al.* (1963). Over a range from a large vessel of 1,000 μm in radius to a terminal branch of 10 μm, the blood pressure of the portal vein was demonstrated to drop by only a few mmHg, a great difference from that of the hepatic artery.

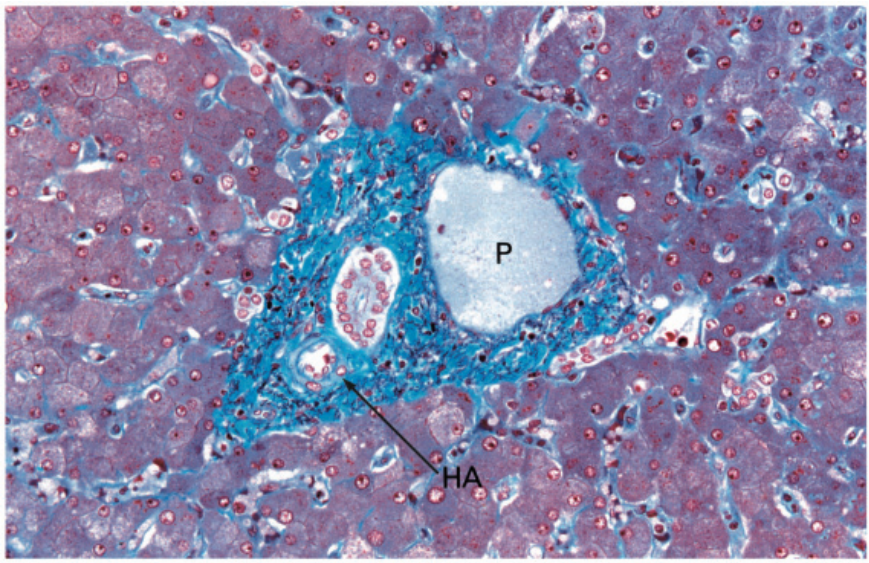

Fig. 3-11. Microscopic appearance of a portal tract of normal human liver. P: portal vein. HA: hepatic artery. The artery is equipped with thick layer of smooth muscles which however are not recognizable in the portal vein. Elastica-Goldner stain.

vein and hepatic artery by quantitative treatment of methacrylate casts of these vessels. The study, performed according to the mathematical theorem developed by Suwa *et al*. (1962), demonstrates that the pressure gradient of portal blood flow is incomparably smaller.

Moreover, the blood flowing into the liver has to be distributed to the peripheral lobules sufficiently uniformly over this large organ. This is a critical requirement to be satisfied so that the portal blood, after flowing into the liver, may make sufficient contact with the intralobular hepatocytes. Otherwise, the liver would be unable to function as the central organ of metabolism. Particularly, one has to keep in mind that the liver plays crucial role in detoxifying noxious substances absorbed in the GI tract and carried via the portal vein. If there were unevenness in the density at which portal blood irrigates the hepatic parenchyma, allowing a part of blood to pass through the organ without making sufficient contact with hepatocytes, the result would be a hepatic insufficiency, although various in its clinical seriousness.

In this connection, let us recall what was discussed in Chapter 1. It was shown that the systemic arteries have in the peripheral arterioles an enormously thickened medial coat, and that these hypertrophic smooth muscles are mainly assigned to regulate the peripheral flow of blood. However, the intrahepatic portal venous tree that is a low-pressure vessel has no such regulatory apparatus even at the periphery. Figure 3-11 presents a microphotograph of portal tract from a normal liver of human, and one can see that while the small hepatic artery (HA) is equipped with hypertrophic smooth muscles, no muscular component is recognizable in the wall of the small portal vein (P).

The significance of isodistant vasculature: two vascular models (Figs. 3-12, 3-13, 3-14)

The uniquely isodistant relation of the portal and hepatic venules shown above seems to be the structure that satisfies the requirement which the liver has in achieving its circulatory and metabolic functions. In other words, one can find in the hepatic

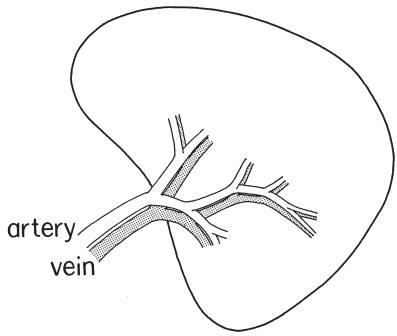

Fig. 3-12. A schema illustrating arteries and veins entering and going out of an organ, both running in parallel. In most organs, arteries and veins run and divide toward the periphery, retaining the contiguous relation.

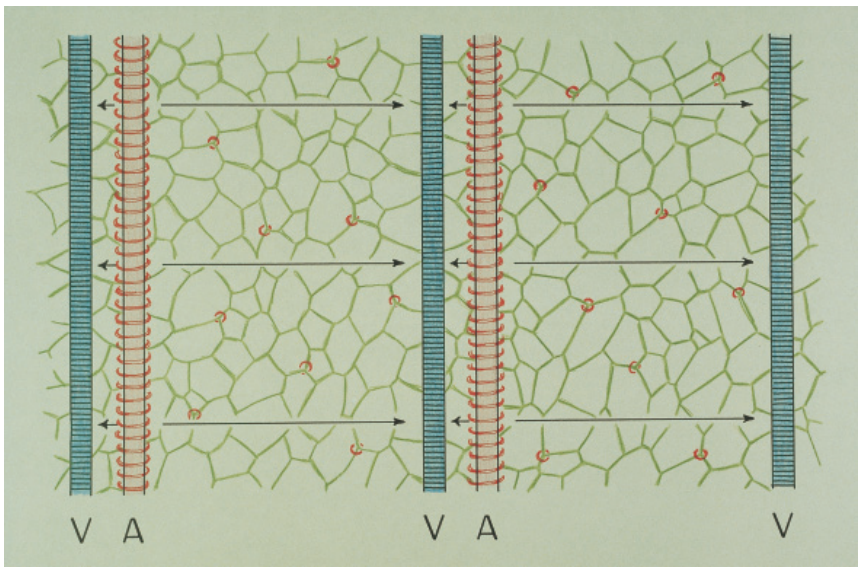

Fig. 3-13. Microcirculation Model 1, with contiguous arrangement of terminal arteries (A; or afferent vessels like portal vein), red, and terminal efferent veins (V), blue. Capillary network is shown in green. Under this vasculature, the distance of capillary flow routes greatly varies, and so does the flow resistance. This inequality has to be compensated by active flow regulation on the part of vascular smooth muscles which are illustrated with either red spirals surrounding the terminal arteries or red rings sporadically found around capillaries.

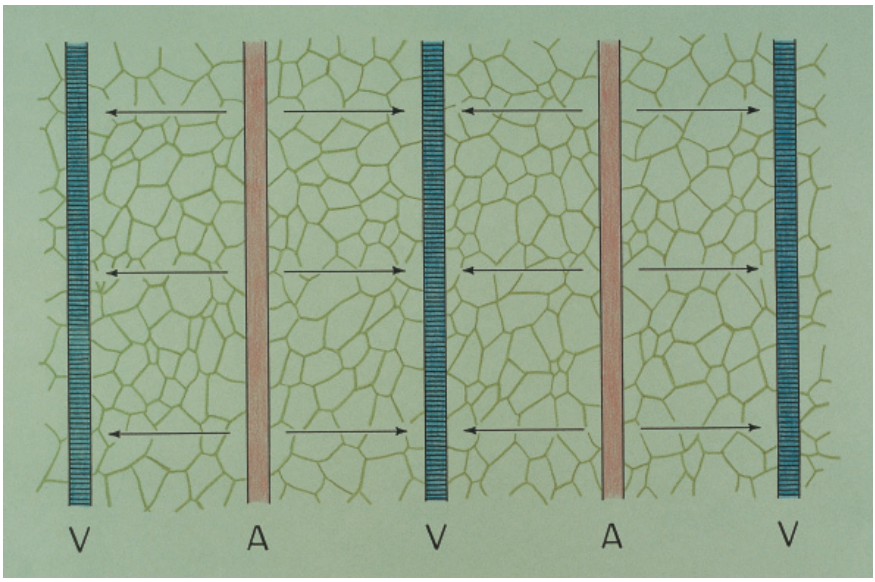

Fig. 3-14. Microcirculation Model 2, with isodistant arrangement of terminal afferent (A) and efferent (V) vessels. Here the distance of capillary flow routes, and also the flow resistance, is ensured to be fairly uniform.

microvasculature a sort of "adequate design," the optimum structure-function correlation. This will be understood by making the following ideal experiment.

Usually, an organ has a hilus where an artery enters and a vein leaves the organ but they do so closely in parallel as in Fig. 3-12. This relation is brought into the organ, where arteries and veins run and divide, maintaining the close adjacency. What if, however, this contiguity should be kept down to their terminal region where they are joined with the capillary network? Here, one will have to expect a difficulty in the tissue microcirculation, for the following reason.

Figure 3-13 is a schema of contiguous vasculature. Here we assume that the space between the small arteries and veins (more generally, afferent and efferent vessels) is uniformly filled with capillary network (green). If arteries and veins are located in close adjacency like the figure, a great inequality occurs in the length of flow routes through capillaries, and produces shortcircuited flow at the places of contiguity. Therefore, under this vasculature, blood cannot be distributed uniformly over the tissue, unless there is a correcting mechanism which actively regulates and redistributes blood flow. As is well known, it is the sphincter action of vascular smooth muscles that is responsible for this regulation, i.e., the medial smooth muscles of small arteries and arterioles, and also the smooth muscle cells sporadically found in capillaries. The seemingly luxurious muscular coat of the arterioles as demonstrated by the elevated D/R ratio (Fig. 1-9) must have been expressing the extremely vigorous activities of these vessels assigned to regulate the tissue blood flow. Only with the combined activities of these regulatory apparatuses, will the tissue blood flow be equalized over the

whole region.

However, we have another extreme too, as in Fig. 3-14. Here, the terminal arteries and veins (or, afferent and efferent vessels) are keeping a uniform distance. Under this isodistant pattern, the length of capillary routes becomes uniform. It would ensure a uniform resistance to flow, and ensure a distribution of blood at a uniform density, even if the vessels are not equipped with any apparatus for regulation. Since in the liver, the peripheral portal veins are not equipped with smooth muscular coat and are considered to be devoid of regulatory function, it appears that this isodistant relation may be the very structure required by this organ.

Organ difference in microvasculature: functional significance (Table 3-1)

We now understand that in the organ circulation there is an aspect, in which the flow dynamics depends on the vascular architecture. This is an aspect of microcirculation that has nothing to do with the structure of capillary network itself. As summarized in Table 3-1, in organs having an isodistant vasculature, a uniform blood flow in the tissue is likely to be realized even in the absence of regulation. In contrast, in an organ with a contiguous architecture, an active regulation is indispensable. As we will see, the isodistant group includes the liver and the lung. Significantly, these are organs supplied by a low pressure vessel, namely, the liver by the portal vein and the lung by the pulmonary artery. The wall of intrahepatic portal venules has practically no smooth muscles. In the pulmonary arteries, where the mean blood pressure at the trunk does not exceed 15 mmHg, smooth muscular coat is only poorly developed in the peripheral branches (see Fig. 1-10). On the other hand, the contiguous group includes the myocardium and the renal cortex, and here, an active regulation is considered to prevail.

However, in gaining more insight into the structure-function correlation in this context, what we have to do first of all is to define accurately the degree to which the vascular architecture of an organ is isodistant or contiguous, instead of intuitively judging the pattern by inspection. Then, how can we describe in quantitative terms the difference in the vascular pattern? With what parameter can we measure the grade of isodistance or contiguity in 3-D? Here we face a problem of 3-D quantification.

Table 3-1. The pattern of mircovasculature and the microcirculation considered to dominate under the vasculature. The organ difference.

Vasculature	Flow dynamics	Organ examples	Inflow vessel
Isodistant	Non-regulatory	Liver	Low pressure system
		Lung	
		. . . . .	
		Brain	
		. . . . .	
Contiguous	Regulatory	Myocardium	High pressure system
		Renal cortex	

c) Quantitative expression of vasculature pattern

The concept of *L*: 3-D distance distribution (Figs. 3-15, 3-16)

Figure 3-15 illustrates a geometric model the author proposed for the quantification of vascular patterns. Let us take a point P randomly in an organ. Suppose that we can determine L_a, the shortest distance from P to the nearest artery (or afferent vessel), and also L_v, that to the nearest vein (or efferent vessel). Then we define the distance *L*,

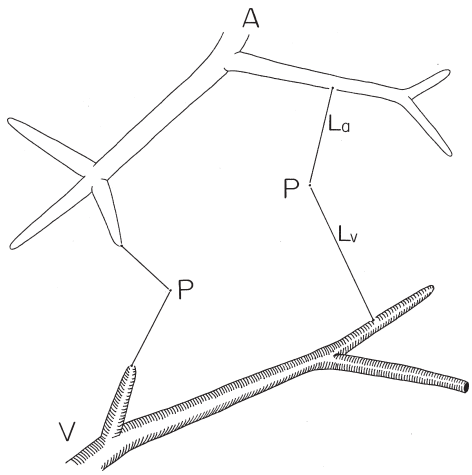

Fig. 3-15. The concept of *L*, the length of the shortest capillary flow route via a sampling point P randomly taken in the space. The length *L* changes if P is moved around in the space, for example to the other point in the left part of the figure. Reproduced from Takahashi (1970): Tohoku J exp Med 101, pp. 127.

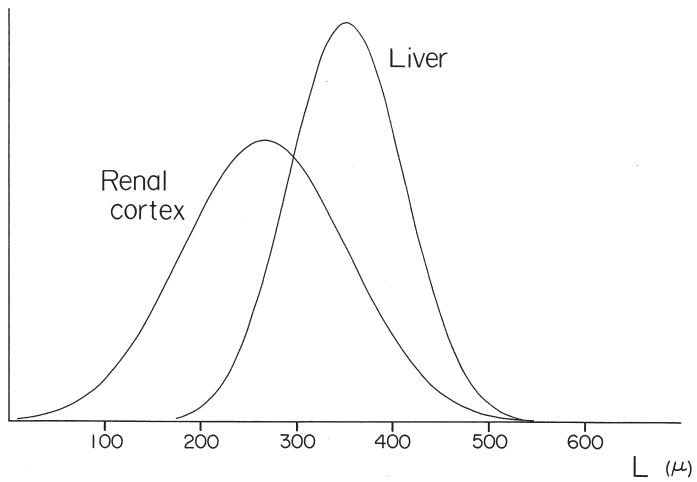

Fig. 3-16. The distribution of *L* obtained from measurement of a large number of points in normal liver and kidney. In the liver, the dispersion of *L* is smaller than the kidney, showing that the pattern of vasculature is more isodistant. Reproduced from Takahashi (1970): Tohoku J exp Med 101, pp. 127.

the sum of L_a and L_v, as the length of the shortest capillary route via P. This length changes when the point P is moved around in the organ, for example to the left-sided point in the figure. Accordingly, if we set a sufficiently large number of points randomly in the organ and measure L, then it will become a statistical quantity.

Consider that in an organ, the length L was measured for hundreds of points and the dispersion of L was calculated. In Fig. 3-16, results from two organs are shown for comparison. If the dispersion of L proved to be comparatively small as in the liver, the vasculature in the organ is likely to be more isodistant. In contrast, the larger the dispersion, the more contiguous vasculature is suggested to exist. Thus, in this context, what we have to obtain by morphometry is the mean and the dispersion of L.

Three-D distance distribution: measurement (Figs. 3-17, 3-18, 3-19, 3-20)

In practice, measurement of L was designed to perform on serial microscopic sections. In an organ, 300 to 400 sampling points were set by "tessellation" on a level of serial sections as schematized in Fig. 3-17. In estimating the mean and variance of L, we cannot rely on stereology, as shown by DeHoff in the classification of geometric properties (Table 2-2), in which the present task belongs to "spatial distribution information."

I thus undertook a manual measurement. While graphically reconstructing small vessels, the shortest distance from P to a nearest vessel was determined by calculating the distances sequentially on serial sections. L, which is a 3-D distance, was determined as in Fig. 3-18 by measuring the xy-distance on a stack of serial pictures and calculating the z-distance from the number of serial sections. As might be expected, this was quite a time-consuming work.

But now we have a computer-assist for this measurement thanks to the programming by T. Chiba (Takahashi and Chiba, 1990). From a set of serial sections, blood

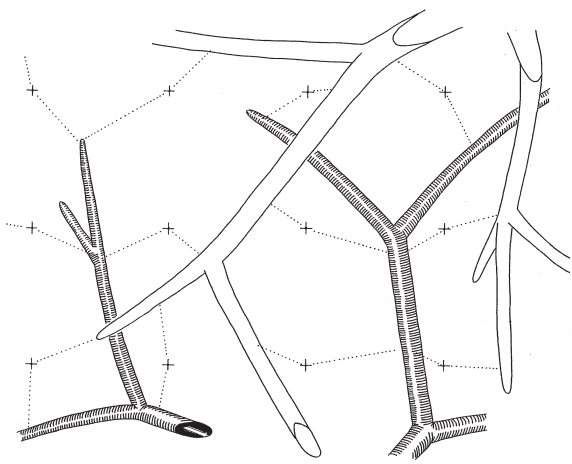

Fig. 3-17. Setting of sampling points for the measurement of L. In one of the serial sections, hundreds of points are set by "tessellation," i.e., at the crossing points of orthogonal parallel lines. Reproduced from Takahashi (1970): Tohoku J exp Med 101, pp. 128.

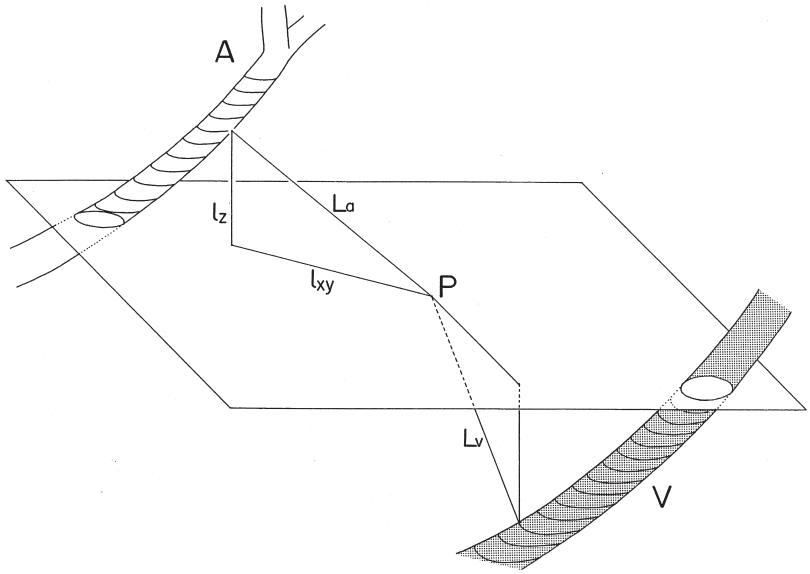

Fig. 3-18. A schema showing how *L* was obtained by manual measurement. The length of the shortest flow route *L* was obtained by comparing the values among several steps of serial sections. At each step of serial sections, *L* was calculated from $L^2 = lxy^2 + lz^2$, where *lxy* is the distance from P to the nearest vessel projected on the *xy* plane. *lz* is given by the number of serial sections. Reproduced from Takahashi (1970): Tohoku J exp Med 101, pp. 128.

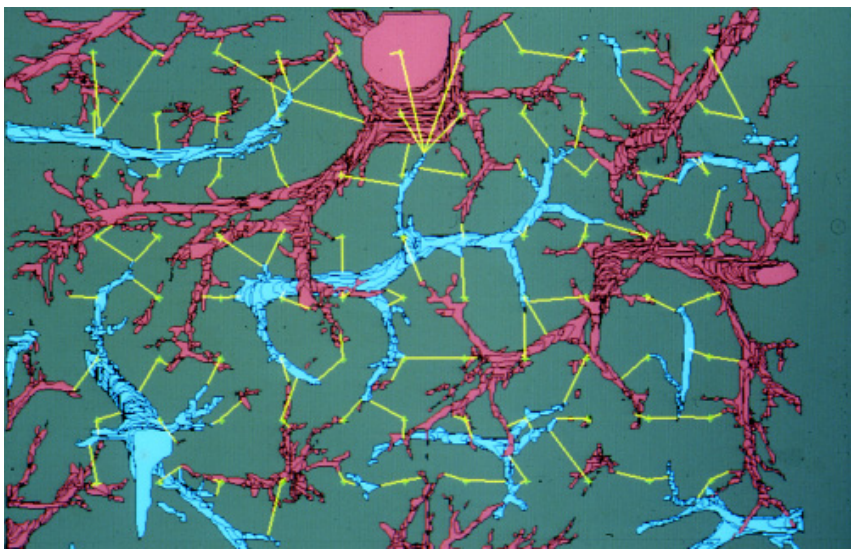

Fig. 3-19. Computer-aided measurement of *L*. The yellow lines are the shortest capillary routes selected by computational geometry. Reproduced from Takahashi and Chiba (1990): Science on Form II, pp. 24.

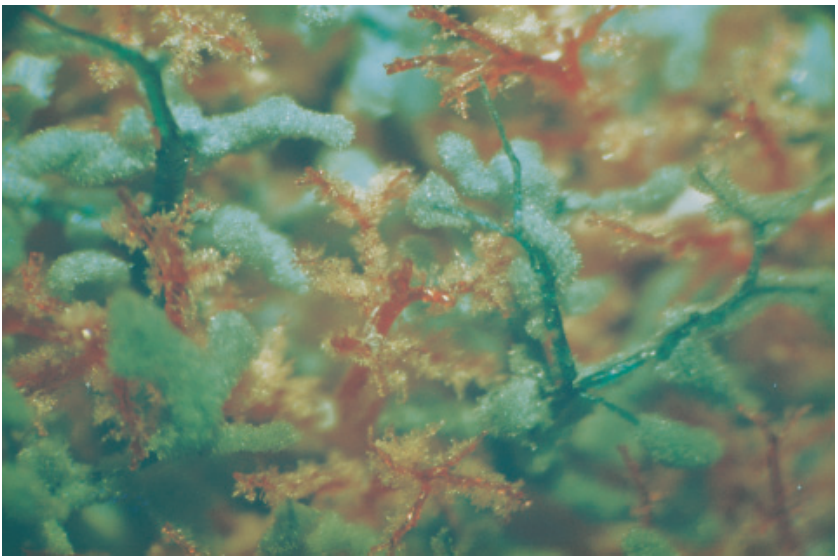

Fig. 3-20. A methacrylate cast of liver microvessels. Red are the portal, and blue are the hepatic veins. Here the arrangement of vessels may seem suggesting the presence of isodistant vasculature, but a cast does not allow to compare the 3-D vascular pattern in quantitative analytical terms.

vessels are digitized at every step, and we have a whole set of 3-D structural data in a hard disc. Figure 3-19 is an example in a normal liver (portal vein, red; hepatic vein, blue). Here one can see 88 test points, and the yellow lines are the shortest routes calculated.

The microvasculature of an organ may be visualized much more easily by preparing a corrosion cast than performing 3-D reconstruction of microvessels. Figure 3-20 presents an example where the portal veins were injected with red resin and the hepatic veins with blue one. Here too, one can see the isodistant spatial arrangement of the vessels as seen in Fig. 3-7. Despite its easy accessibility, however, a resin cast hardly serves if one attempts to quantitatively analyze the 3-D microvasculature of organs, for example by measuring the 3-D distance from a random point to the vessels. It is for this reason that the author preferred serial sections analysis to the use of vascular casts.

Distribution of L in normal liver (Fig. 3-21)

Figure 3-21 demonstrates the result of measurement in a normal liver, in this case on 325 points. Clearly, the spatial distance L follows a normal type distribution, and so does it in any organ examined. The mean L is calculated at 352 μm, which corresponds to the mean length of sinusoidal routes because most of the sinusoids appear taking approximately the shortest linear course towards the central vein. It is noteworthy that the value is in good accordance with the mean lobular radius obtained in the foregoing chapter by applying stereology to a cylindrical model (Fig. 2-39).

As explained, the aim of this analysis has been to compare the dispersion of L among organs. But, the standard deviation of L was not an appropriate parameter,

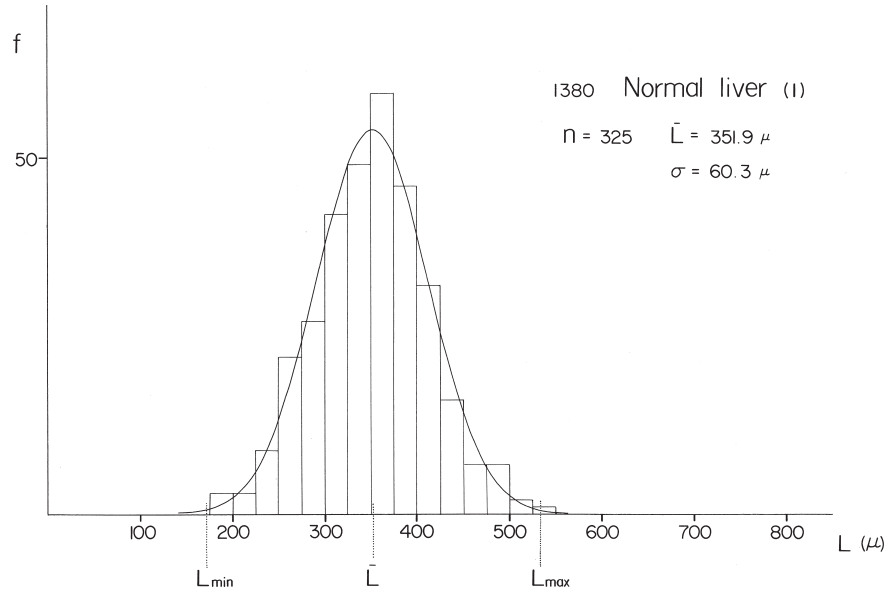

Fig. 3-21. Distribution of L in a normal liver based on a measurement with regard to 325 sampling points. Note quite a normal type distribution. The mean L is calculated at 352 μm, a value exactly corresponding to the mean radius R of hepatic lobule obtained stereologically (Fig. 2-39). The dispersion of L is expressed by the "vasculature index," the ratio of L_{max}/L_{min}, with both L_{max} and L_{min} defined at 3σ levels, i.e., the mean $L \pm 3\sigma$. In the liver, the index proved to be 3.0, the minimum of the organs examined, showing that indeed, the organ is equipped with a microvasculature that is the most isodistant. Reproduced from Takahashi (1970): Tohoku J exp Med 101, pp. 129.

because there was a certain between-organs difference in the mean L. Therefore another method was introduced. Since the distribution of L could be approximated by a normal distribution, its upper and lower limits were defined at 3σ levels, the mean $\pm 3\sigma$. Here, if the ratio of the maximum L (mean $L + 3\sigma$) to the minimum L (mean $L - 3\sigma$) is calculated, it would serve as an index of vasculature, describing to what degree the afferent-efferent distance is uniform. The smaller the index, the more uniform the distance, and vice versa. In the normal liver of Fig. 3-21, we obtained an index value of 3.1. We examined a normal liver from another patient and obtained an index of 2.9. Thus, the quantity for the normal liver proved to be about 3.0.

Organ difference in the distribution of L (Table 3-2)

In Table 3-2, the index values are compared among five organs, the liver, lung, cerebral cortex, myocardium and kidney. It is shown that the value of 3.0 of the liver is by far the smallest, and demonstrates that certainly, this organ is equipped with a vasculature prominent in isodistance. It exceeds 50 in some organs of systemic circulation.

Table 3-2. Comparison of vasculature index L_{max}/L_{min} among the organs examined. Note that in the liver the index value is the smallest, showing the most isodistant vasculature among the organs.

Organ		mean L	σ	L_{max}	L_{min}	L_{max}/L_{min}
Normal liver	(1)	352	60	533	171	3.1
	(2)	419	69	625	214	2.9
Lung		218	50	368	69	5.4
Cerebral cortex		165	45	299	31	9.7
Myocardium		168	54	330	6	51.1
Renal cortex		267	86	525	10	54.7
Chronic hepatitis	(1)	377	129	919	155	5.9
	(2)	350	129	853	144	5.9
	(3)	577	135	1466	227	6.5
Liver cirrhosis	(1)	528	175	1770	158	11.2
	(2)	572	181	1995	164	12.2

Normal liver: a re-consideration upon microphotograph (Fig. 3-22)

The liver of man comprises a uniformly continuing parenchyma as in Fig. 3-22. Here the blood vessels seem to be enjoying the greatest freedom with which they spread in the space, realizing an ideal isodistant relation. Perhaps the structure of lobules as polyhedra packed in the space may have been another aspect of this extremely isodistant vascular arrangement. In the figure, a 2-D section of the liver, the contours of lobules as packed polygons are visualized on account of mild hydropic changes of hepatocytes in the central zone of lobules.

Still, we have a question. What is responsible for the variety of 3-D vasculature patterns? From a purely microcirculation point of view, the isodistant pattern must be the most advantageous, since it ensures the most stable and uniform distribution of blood. Nevertheless, it is allowed to exist only in the liver, and to lesser degree, in the lung. Why such an organ difference? Let us consider about the background of this variety by comparing the liver with the lung, as in the following.

d) Why does the vascular pattern differ among organs?

Three-D vasculature of lung (Fig. 3-23)

Figure 3-23 is a manually performed reconstruction of small pulmonary arteries and veins in a normal human lung. At a glance, the vascular pattern seems to be isodistant to a similar degree as in the liver. However, there is a small difference. The terminal vessels tend to curve so as to wrap spaces about 500 μm in diameter, as depicted by dots in the upper, middle left and lower left parts of the figure. By closer observation, one may realize that similar spaces are ubiquitous, and the whole lung tissue consists of an assembly of such spaces. In terms of microanatomy, each of these

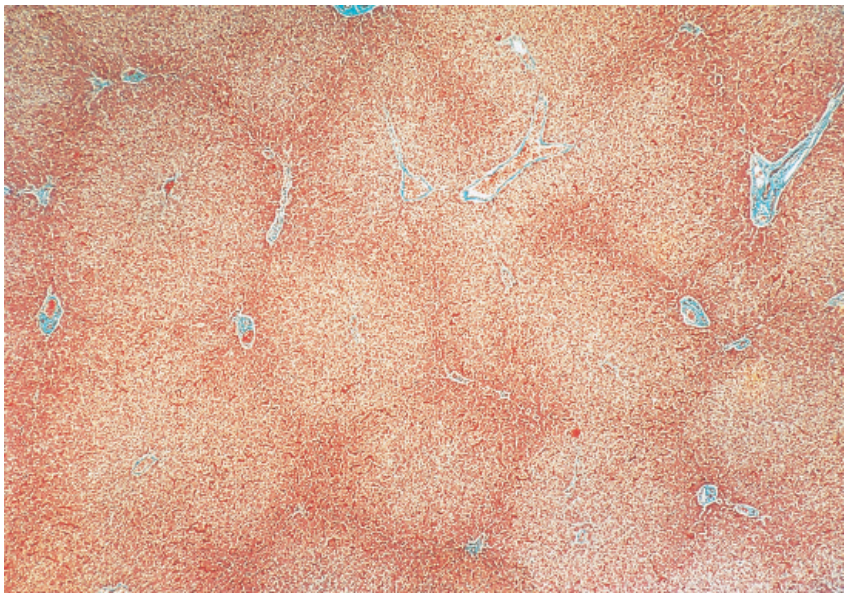

Fig. 3-22. A microphotograph of human liver. The polygonal lobules are visualized on account of mild hydropic changes of hepatocytes in the central zones of lobules. Elastica-Goldner stain.

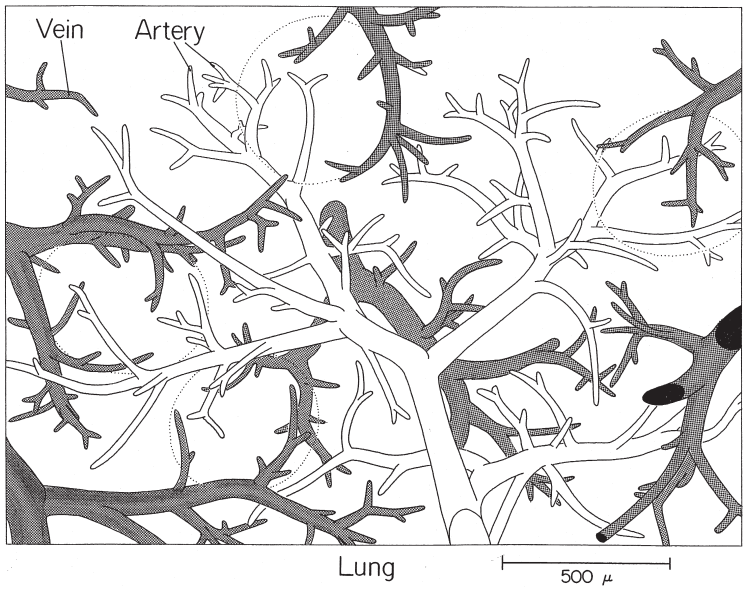

Fig. 3-23. The 3-D microvasculature of the human lung, visualized by manual reconstruction. The vessels shown white are pulmonary arteries and those shaded are pulmonary veins. The pattern of vasculature seems to be isodistant, but there is a difference from the liver. As denoted by dots, the small lung vessels tend to wrap a space 0.5 to 0.6 mm in diameter, which anatomically corresponds to either an alveolar sac, or a segment of alveolar duct. Reproduced from Takahashi (1970): Tohoku J exp Med 101, pp. 131.

spaces corresponds to either an alveolar sac or a segment of alveolar duct, including the alveoli opening there. In contrast to the liver where the afferent and efferent vessels penetrating the parenchyma can take any position, an alveolar sac as well as alveolar duct of normal lung is an air space which does not allow arteries or veins to enter its interior as a naked vessel not contained in alveolar septum. While in the 3-D picture of Fig. 3-23 the lung vessels seem to be arranged in an isodistant fashion, in reality, it is only among the vessels enclosed within the alveolar septa that the isodistance is realized.

Three-D vasculature: difference between the lung and liver (Figs. 3-24, 3-25)

A slight deviation in the lung from the highest regularity is reflected in the distribution of *L* (Fig. 3-24). Here the index of vasculature is 5.4, a little larger than in the liver where it was 3.0. The background underlying this difference discloses itself in the microstructure of lung as shown in the next figure.

Figure 3-25 is a sketch of lung tissue and here, one thing is to be pointed out. The small pulmonary arteries (white), as well as veins (black), are all deployed in the wall of the airways. But the airways from bronchi to bronchioles to ductus alveolaris (d.a.) to alveoli are all organized into a tree, following a principle that is considered to give the lung a condition optimal for ventilation function (One may have a glimpse of what the principle looks like, in the studies published by Kitaoka *et al.*, 1999). In other words, in the lung, the degree of freedom assigned to the structure of blood vessels is correspondingly reduced.

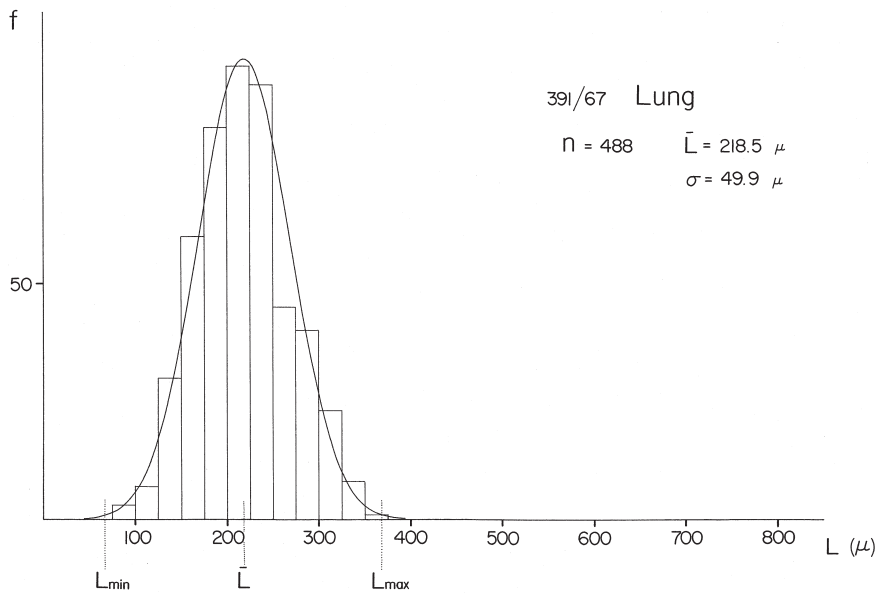

Fig. 3-24. The distribution of *L* in a normal human lung. A fairly isodistant pattern with comparatively small dispersion of *L*, but the vasculature index is 5.4, a little higher than in the liver. Reproduced from Takahashi (1970): Tohoku J exp Med 101, pp. 131.

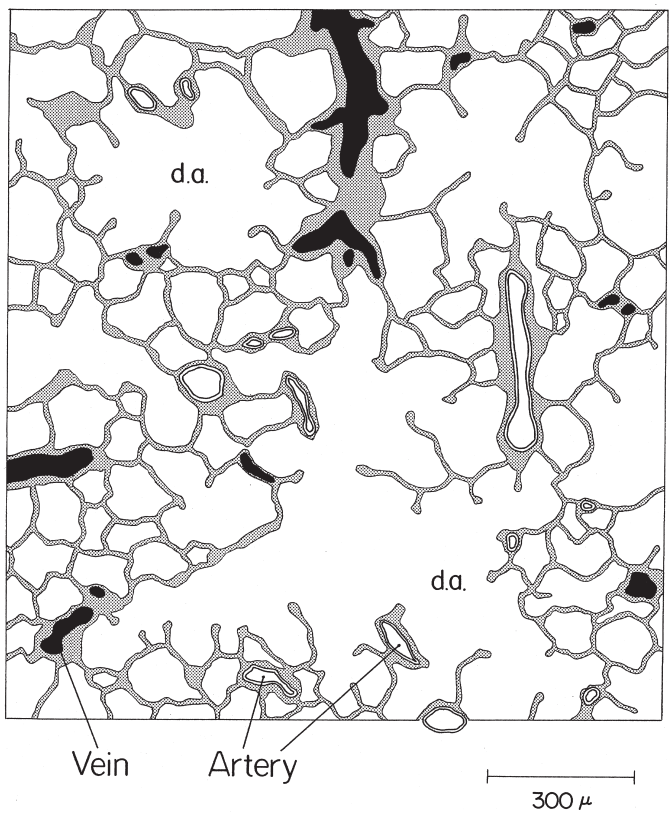

Fig. 3-25. On one of the serial sections of lung, the microscopic picture was projected on a sheet of paper, and the contours of airways, alveoli and blood vessels were drawn by tracing. d.a.: ductus alveolaris. Of the blood vessels, pulmonary arteries are shown white, pulmonary veins black. Reproduced from Takahashi (1970): Tohoku J exp Med 101, pp. 133.

The isodistant vasculature and the structure of liver parenchyma (Figs. 3-26, 3-27)

Based on the above discussion, let us re-examine the parenchymal structure of the liver. The liver is the central organ of metabolism, but at the same time it works as an exocrine gland secreting bile as stressed by Rappaport. Figure 3-26 is a microphotograph of human liver impregnated with silver. There are capillaries densely connected to form a fine network. Flanked by capillaries are hepatocytes arranged in the form of one-cell thick plates, that are forming another network intertwined with the capillaries.

Figure 3-27 is a schema explaining the 3-D structure of liver parenchyma which is penetrated by a network of capillaries (s: sinusoids). The hepatocytes forming one-cell plates secrete bile into the bile canaliculi (bc), another fine network extending along the border between a pair of neighboring hepatocytes. This is a unique type of

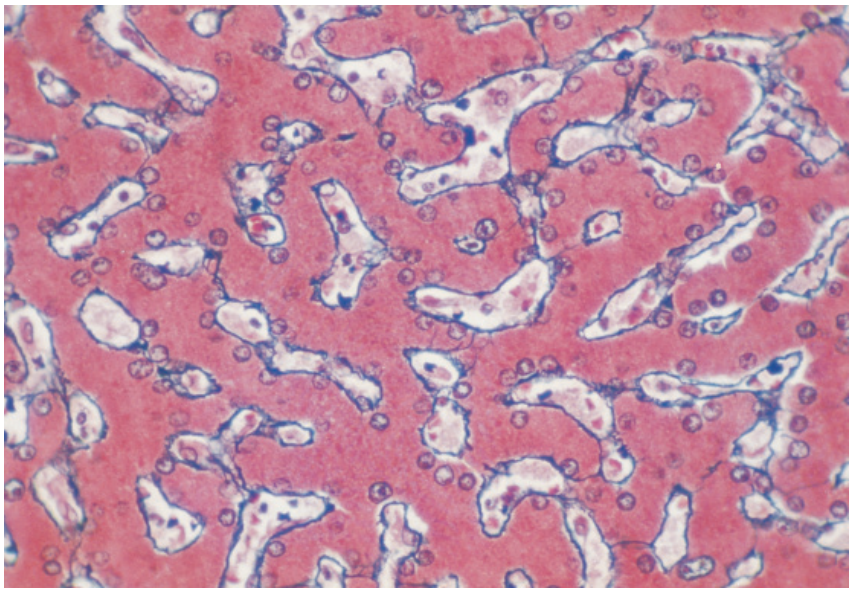

Fig. 3-26. High power microscopic appearance of normal hepatic parenchyma of man. Hepatocytes are arranged into forming thin, one-cell thick plates, the liver cell plates, which are organized into a fine 3-D network that are closly intertwined with the capillary network, the void spaces. Gomori's silver stain.

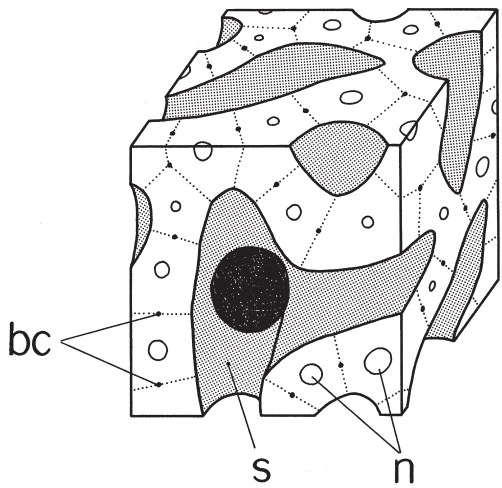

Fig. 3-27. A schema of 3-D parenchymal structure of the liver. The mass of liver cells is densely penetrated by capillaries, also called sinusoids (s), that leave the liver cells in the form of one-cell plates. Liver cells secrete bile into bile canaliculi (bc), another fine network extending along the border between a pair of neighboring liver cells.

exocrine gland called a netlike gland where no such hierarchic arborization exists as found in the ductal tree of usual gland. Thus, although the liver is a sort of exocrine gland, it presents quite a specialized one, requiring little if any structure of its own.

An organ is composed of different functional systems (Fig. 3-28)

The regular isodistance may be the pattern of vasculature ideal for microcirculation, because it ensures uniform irrigation of blood even in organs where the peripheral vessels are not equipped with apparatuses for blood flow regulation. However, this ideal type of vasculature cannot always be realized, because every organ has functional systems other than the vascular system, each of which requires a structure most adequate for its function. For example, the lung has, besides the blood vessels, the airway system which requires a design adequate for its ventilation function. However, the different systems have to co-exist in a limited space somehow. The circumstances are the same in any organ. Besides the vascular system, the renal cortex has nephrons, the myocardium has a system of heart muscles, and they are all arranged in the space according to a rigorous rule. Thus, we find in actual organs a vascular pattern that is more or less contiguous, but this seems to be a result of compromize. Why in the liver the most ideal isodistant vasculature is realized may be understood if the other functional system of the liver, the bile-secreting gland system, is considered. As above, we find in the liver quite a specialized gland, requiring little if any structure of its own, thus allowing the vascular system to enjoy the highest degree of freedom to spread in the space and create a vasculature which is the most optimal for microcirculation. Figure 3-28 is a schema in which the transverse length for each of the rows is meant to express, in arbitrary fashion, the degree of freedom assigned to the functional system to form a structure adequate for its function.

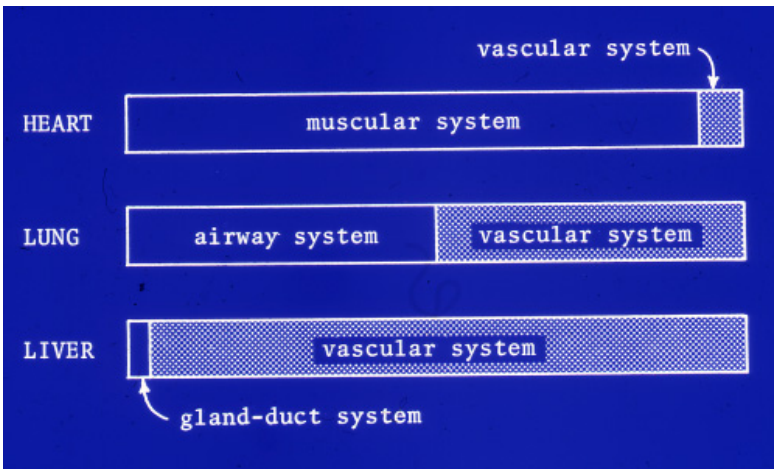

Fig. 3-28. A schematic presentation showing that an organ comprises several functional systems, and that to each of the systems, various degree of freedom is assigned with regard to the structure. For explanation see the text.

e) Pathogenesis of hepatic failure in cirrhosis

The structure of cirrhosis: 2-D and 3-D (Figs. 3-29, 3-30)

Now let us see how the above discussion helps us understand why livers with cirrhosis are apt to develop hepatic failure, one of the major causes of death among cirrhotic patients. Figure 3-29 is a microphotograph of cirrhotic liver from a patient suffering from chronic hepatitis C for about 20 years. Here it is shown that a cirrhotic liver consists of two elements: the round nodules stained red-brown, and the interstitial zones stained green. The interstitium is the scar zone left after the hepatocytes were destroyed in an active phase of inflammation. The nodules are clumps of hepatocytes that were exempted from damage and are regenerating. In Japan, the prime cause of hepatocellular damage leading to cirrhosis is chronic hepatitis, either B or C, but in Western countries, it is said to be alcohol abuse.

Figure 3-30 is a computer-aided reconstruction of cirrhotic liver. The green wireframes denote the nodular profiles, painted in red are portal veins and those in blue are hepatic veins. One can see that almost all the vessels are running in the interstitium, and at many places they are making anastomoses in the form of P-C, the portal-central, bridging. Obviously, this implies a change from the isodistant vascular pattern of the normal liver into a contiguous pattern. Or in other words, what we find here is a breach of the basic structural principle of the liver. In this situation, the blood flowing in from the portal vein is apt to escape to the hepatic vein without making necessary contact with hepatocytes which are confined in the nodules. Thus the hepatocytes seem to be living upon a small part of portal blood not shunted away through

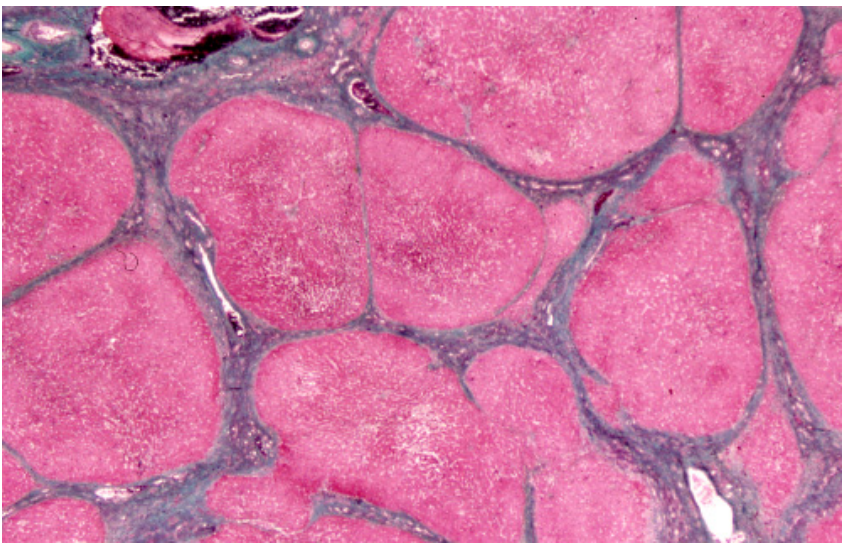

Fig. 3-29. Microscopic appearance of cirrhotic liver that consists of nodules (red-brown) and interstitial zones (green). The nodules are masses of regenerating hepatocytes, and the interstitium is the scar zone left after the hepatocytes were destroyed in the active phase of liver injury. Elastica-Goldner stain.

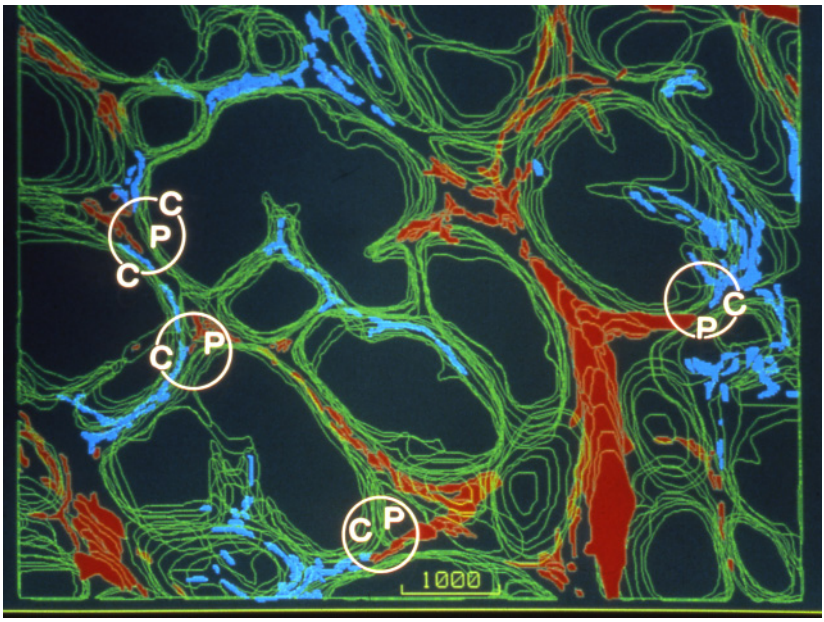

Fig. 3-30. Computer-aided 3-D reconstruction of cirrhosis. The green wireframes denote the contours of nodules. The vessels painted red are portal veins, and those blue are hepatic veins. Note that both of the vessels are mostly running in the interstitial zones. At several places one can find anastomosis between the terminal portal and central (hepatic) veins, forming a portal-central bridging as denoted by PC. This means that the isodistant vasculature of normal liver is lost and replaced by a contiguous arrangement.

the interstitium. In consequence, the liver cannot sufficiently detoxify the portal blood, and thus, hepatic failure ensues. And now we understand that all these are attributable to the deviation of vasculature from the normal isodistance.

Vasculature change in cirrhosis described by the distribution of *L* (Fig. 3-31)

Now that the development from normal livers over chronic hepatitis to cirrhosis is reduced to a change of vasculature from isodistance to contiguity, we can assess the progression with the index of vasculature. Figure 3-31 presents the result of measurement of *L* in three livers with chronic hepatitis and two cirrhotic livers, combined with the two normal livers shown above. One can see the distribution of *L*, while narrow-ranged in normal livers (green), become progressively flattened over chronic hepatitis (yellow) to cirrhosis (red). The index value which was normally 3.0, is elevated to 10 or more in cirrhosis (see Table 3-2, p. 87). Thus, the spatial distance distribution allows us to describe the degree to which the microvasculature is deviated from its normal state. How can the deviation occur? This is understood by studying livers with diseases preceding cirrhosis, which will be shown in Chapter 6.

In the present chapter it might appear that 3-D reconstruction was used only as a tool for obtaining the index of vasculature, but while performing reconstruction, a

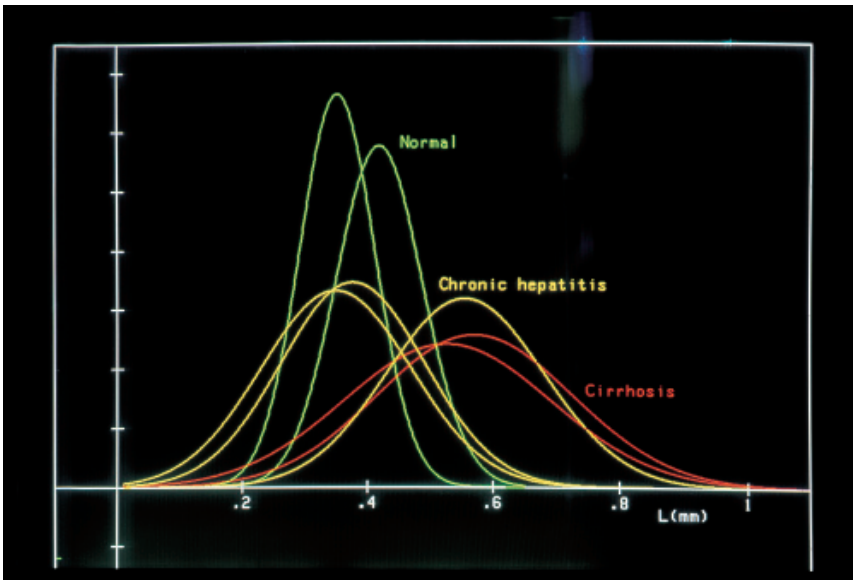

Fig. 3-31. The distribution of *L* was examined in two normal livers (green), three livers with chronic hepatitis (yellow) and two cirrhotic livers (red). Note that the dispersion of *L* becomes increasingly large with the progression of disease from chronic hepatitis, a pre-cirrhosis, to cirrhosis.

variety of knowledge and concepts on the structure of various organs have been obtained. In the next chapter, the technique of 3-D structural analysis will be introduced. Let us see how it can be applied to various problems of pathology.